Editors' Suggestion | Featured in Physics

Near Ground-State Cooling of Two-Dimensional Trapped-Ion Crystals with More than 100 Ions

Elena Jordan,[1,*] Kevin A. Gilmore,[1,2] Athreya Shankar,[2] Arghavan Safavi-Naini,[2] Justin G. Bohnet,[1] Murray J. Holland,[2] and John J. Bollinger[1]

[1]*Time and Frequency Division, National Institute of Standards and Technology, Boulder, Colorado 80305, USA*
[2]*JILA, NIST, and Department of Physics, University of Colorado Boulder, Boulder, Colorado 80309, USA*

(Received 18 September 2018; published 7 February 2019)

We experimentally study electromagnetically induced transparency cooling of the drumhead modes of planar two-dimensional arrays with up to $N \approx 190$ Be^+ ions stored in a Penning trap. Substantial sub-Doppler cooling is observed for all N drumhead modes. Quantitative measurements for the center-of-mass mode show near ground-state cooling with motional quantum numbers of $\bar{n} = 0.3 \pm 0.2$ obtained within 200 μs. The measured cooling rate is faster than that predicted by single particle theory, consistent with a quantum many-body calculation. For the lower frequency drumhead modes, quantitative temperature measurements are limited by frequency instabilities, but near ground-state cooling of the full bandwidth is strongly suggested. This advance will greatly improve the performance of large trapped ion crystals in quantum information and metrology applications.

DOI: 10.1103/PhysRevLett.122.053603

Motivated by metrology and quantum informatic applications, along with the fundamental interest in controlling quantum degrees of freedom (d.o.f.), the preparation of mechanical oscillators close to their quantum mechanical ground state has been an active pursuit for three decades. Early examples include cooling the high-frequency cyclotron motion of a single trapped electron [1] by refrigeration (i.e., coupling it to a cold environment), and laser sideband cooling the lower frequency motion of single trapped ions [2] and trapped neutral atoms [3]. More recently, single, high-Q modes of macroscopic mechanical oscillators have been cooled close to the ground state, either by refrigeration [4], or through sideband cooling [5,6].

Simultaneously ground-state cooling many modes of a macroscopic resonator or a large trapped-ion crystal remains a challenge. Traditional sideband cooling has been extended to cooling multiple modes of small ion crystals [7,8], but does not scale well as the number of ions and modes increases. Electromagnetically induced transparency (EIT) cooling [9–13] shows promise for greatly extending the number of modes or motional d.o.f. that can be ground-state cooled, as was shown for the radial modes of a linear string of 18 ions [14]. Here we demonstrate near ground-state cooling for all the axial drumhead modes of two-dimensional crystals with more than 100 ions, giving us exquisite quantum control of a mesoscopic system. Our experiments are consistent with our numerical results that are discussed in detail in Ref. [15]. Aside from the intrinsic interest in preparing larger mesoscopic systems close to their quantum mechanical ground state, ground-state cooling improves the application of large ion crystals for quantum computation and simulation [16,17] and for weak force sensing [18].

EIT cooling takes advantage of the phenomenon of coherent population trapping [19]. Two energetically lower lying states are coherently coupled by two lasers to the same excited state with equal blue detuning Δ (Fig. 1), so that the ions evolve into a so-called "dark state," where the absorption is zero. A detailed explanation of EIT cooling in a Penning trap can be found in Ref. [15]. The interaction with the lasers modifies the absorption profile. By choosing the powers of the lasers accordingly, the absorption profile

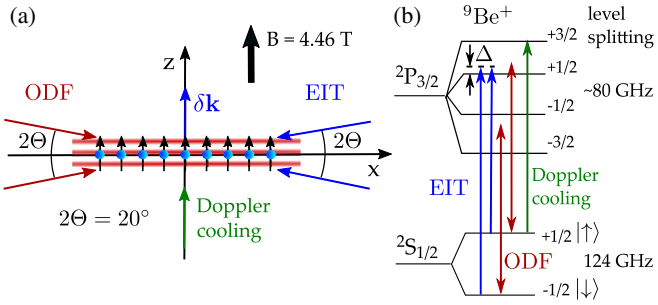

FIG. 1. (a) Schematic laser setup for EIT cooling. The blue spheres represent the ions with their spins (arrows). The beams generating the spin-dependent optical-dipole force (red) cross the ion plane at $\Theta = \pm 10°$, the EIT cooling beams (blue) are counterpropagating relative to the ODF beams. The ODF beams interfere at the position of the ions and form a traveling-wave potential (red fringes). (b) Level diagram of $^9Be^+$ in the 4.46 T magnetic field. The two ODF beams couple to both hyperfine levels of the ground state and have a frequency difference that can be stepped across the drumhead mode frequencies.

can be tailored so that the motion subtracting sideband falls on an absorption resonance and is strongly enhanced, while the motion adding sideband is suppressed. Thus, the ions predominantly scatter a photon while simultaneously losing a quantum of motion, thereby cooling the system [9,10].

Our experimental setup is shown in Fig. 1. We use Doppler laser cooling in a Penning trap, which employs a strong, uniform magnetic field ($B = 4.46$ T) and static electric fields, to form a triangular, single-plane Coulomb crystal with $N \leq 200$ $^9Be^+$ ions [20,21,27,28]. The spin-1/2 d.o.f. is the $^2S_{1/2}$ ground-state valence electron spin $|\uparrow\rangle(|\downarrow\rangle) \equiv |m_s = +1/2\rangle(|m_s = -1/2\rangle)$. At the magnetic field of 4.46 T, the Zeeman splitting of this ground state is 124 GHz. Global spin rotations are driven by a resonant microwave source.

The ions are confined in the direction parallel to the magnetic field by a harmonic electrostatic potential characterized by the center-of-mass (c.m.) frequency $\omega_{\text{c.m.}}/(2\pi) = 1.59$ MHz. The ~0.4 mK Doppler cooling limit for $^9Be^+$ corresponds to a mean phonon occupation number for the c.m. mode of $\bar{n} = 4.6$ [29]. In a direction perpendicular to the magnetic field the ions are confined by the Lorentz force generated by the rotation through the magnetic field. The rotation frequency is controlled with a "rotating wall" potential and set to produce a single plane crystal, typically $\omega_{\text{rot}}/(2\pi) = 180.0$ kHz. For these single-plane crystals, motion along the trap axis (i.e., parallel to $\mathbf{z}$), is described by N axial modes, which we refer to as the drumhead modes [15,27]. Furthermore, there are $2N$ "in-plane modes" associated with motion in the crystal plane [30]. Only the drumhead modes are utilized for applications such as quantum simulation and sensing, and we focus on EIT cooling of the drumhead modes in this Letter.

For EIT cooling, the $|\uparrow\rangle$ and $|\downarrow\rangle$ states are coherently coupled to the $^2P_{3/2}$ $|m_J = +1/2\rangle$ excited state using two lasers with 313 nm wavelength. The two lasers generating the EIT interaction are phase locked with a frequency offset equal to the spin-flip frequency (124 GHz) [21], and intersect with the ion crystal at $\pm 10°$ angles. The collimated beams have a $1/e^2$ diameter of 1 mm providing an approximately uniform intensity over the entire crystal (diameter < 250 μm for $N < 200$). To minimize the interaction of the EIT beams with the in-plane motion, the EIT $\Delta\mathbf{k}$ vector is aligned normal to the crystal plane (parallel to $\mathbf{z}$), with an estimated misalignment of $< 0.2°$. Because the EIT beams are not normal to the single plane crystal, the ion crystal rotation produces a time-varying Doppler shift, which can be several hundred MHz for ions on the crystal boundary, and leads to an effective modulation of the detuning Δ. We chose Δ such that even with the largest Doppler shift the lasers are still effectively blue detuned [15], typically $\Delta = 400$ MHz. We adjust the powers of the EIT beams so that the two Rabi frequencies are equal and the cooling rate for the c.m. mode is maximized [10,21].

Complications such as the time-varying Doppler shifts, insufficient separation of electronic and motional timescales [15], and the simultaneous cooling of a large number of ions interacting through many modes demand careful numerical modeling of the potential efficacy of EIT cooling in a Penning trap. Encouragingly, theory [15] predicts the possibility of near ground-state cooling for all the drumhead modes to $\bar{n} < 0.05$ despite these challenges.

To measure the temperature of the drumhead modes, we couple the axial motion of the ions with their internal spin d.o.f. using a spin-dependent optical dipole force (ODF). The ODF is generated by two interfering off-resonant laser beams with beat note frequency μ_r leading to a traveling-wave potential gradient along the z direction (Fig. 1). The resulting coupling is described by a Hamiltonian of the form $\hat{H} = F\cos(\mu_r t)\sum_{j=1}^{N}\hat{z}_j\hat{\sigma}_j^z$, where F is the ODF amplitude, and $\hat{z}_j$ and $\hat{\sigma}_j^z$ are the position operator and the Pauli spin matrix for ion j, respectively. When μ_r matches a drumhead mode frequency ω_i, spin dephasing proportional to the amplitude of the motion occurs [18]. To measure this spin dephasing, we use the Ramsey-style spin-echo sequence shown in Fig. 2(a). The ions are prepared in the $|\uparrow\rangle$ state, a resonant microwave pulse rotates the spins to align with the x axis, and the ODF produces spin precession. A final $\pi/2$ pulse brings the ions to the $|\downarrow\rangle$ state, if no dephasing occurred. Spin dephasing leads to a finite $|\uparrow\rangle$ state probability (denoted the bright fraction), which we measure through state-dependent resonance fluorescence on the Doppler cooling transition. The method is described in detail in Ref. [31].

Figure 2 shows measurements of the bright fraction with the spin-echo sequence as the ODF difference frequency μ_r is stepped across the c.m. mode frequency $\omega_{\text{c.m.}}$. A clear decrease in the bright fraction is observed when Doppler cooling is followed by EIT cooling, indicating a decrease in dephasing due to the lower c.m. mode temperature. To extract the mean c.m. mode occupation $\bar{n}$, we fit to an analytical expression (see Sec. III.B of Ref. [21]) for the $|\uparrow\rangle$ state probability

$$P(|\uparrow\rangle) = \frac{1}{2}[1 - \exp(-2\Gamma\tau)C_{\text{ss}}C_{\text{sm}}], \tag{1}$$

where the coefficients $C_{\text{ss}} = [\cos(4J)]^{N-1}$ and $C_{\text{sm}} = \exp[-2|\alpha|^2(2\bar{n}+1)]$ describe the phonon-mediated spin-spin interaction and the dephasing that arises from spin-motion coupling, respectively. N is the number of $^9Be^+$ ions and 2τ is the total ODF interaction time. The spin-dependent displacement amplitude α and spin-spin coupling J are functions of τ, the spin-echo π pulse duration t_π, the optical dipole force amplitude F and the frequencies μ_r and $\omega_{\text{c.m.}}$ [21]. We determine F from measurements of the mean-field spin precession [16]. The decoherence rate Γ is mainly due to spontaneous emission and is measured with the same spin-echo

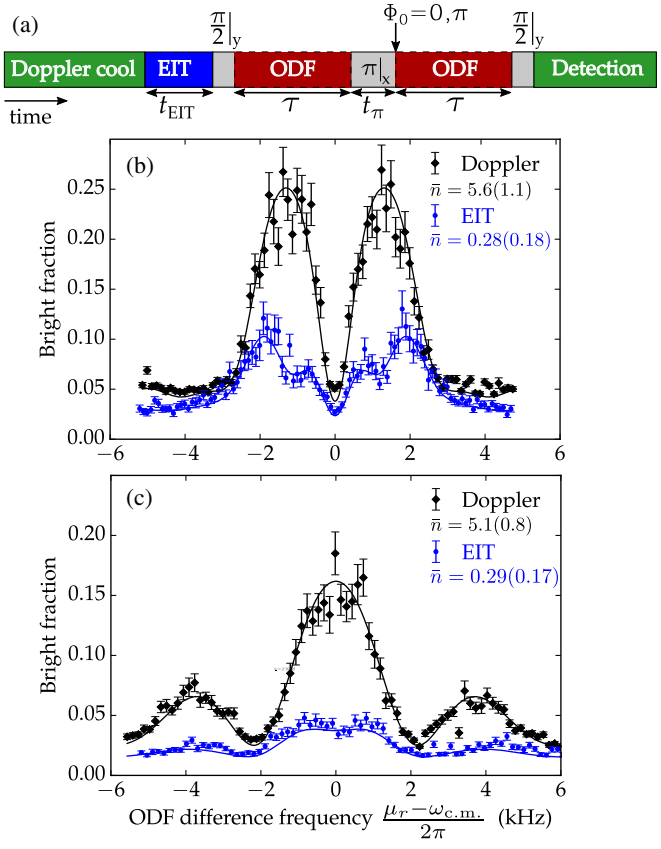

FIG. 2. (a) Experimental pulse sequence. π and $\pi/2$ pulses are implemented with resonant microwaves, Φ_0 is the phase shift between the two ODF pulses. (b) Temperature measurement of the c.m. mode at frequency $\omega_{\text{c.m.}} = 2\pi \times 1.59$ MHz for a crystal with 158 ± 10 ions. The black diamonds are the measured fraction of ions in the $|\uparrow\rangle$ state after Doppler cooling only, and the blue dots after Doppler cooling followed by 200 μs of EIT cooling. The solid lines are least squares fits of Eq. (1) to the data, the fitted mean c.m. mode occupations are given in the legend. Here $2\tau = 500$ μs and $\Phi_0 = 0$. The increased background after only Doppler cooling is due to a larger measured Γ resulting from weak Lamb-Dicke confinement. (c) Same as (b) but with $\Phi_0 = \pi$ and $2\tau = 300$ μs.

sequence but with the ODF beat note μ_r tuned far from any drumhead mode frequencies so that $C_{\text{ss}} = C_{\text{sm}} = 1$.

Figure 2 also shows least-squares fits of Eq. (1) to the experimental measurements where $\omega_{\text{c.m.}}$ and $\bar{n}$ are free parameters. From Eq. (1), the observed signal will include both a temperature-dependent spin-motion component (C_{sm}) and a spin-spin component (C_{ss}) that does not depend on the temperature. For the measurements after only Doppler cooling the signal is dominated by motion-induced dephasing, in contrast to the EIT cooling measurements where the spin-spin component dominates, giving rise to a different line shape. If the ODF phase is shifted by $\Phi_0 = \pi$ for the second arm of the sequence, the line shape is altered and α and J are adjusted accordingly [Figs. 2(a), 2(c) and Ref. [21]].

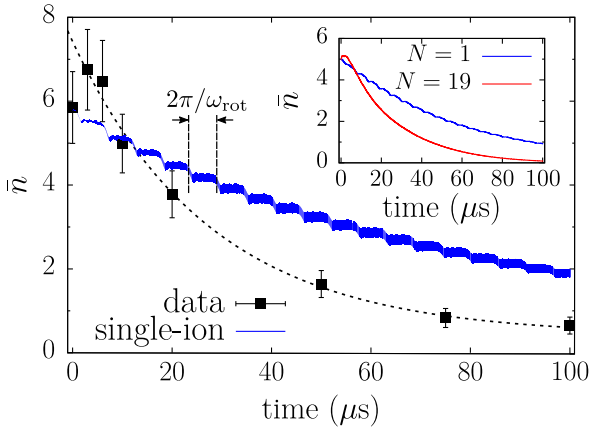

FIG. 3. EIT cooling transient for the c.m. mode of a crystal with $N = 190 \pm 10$ ions. The mean occupation of the c.m. mode $\bar{n}$ is plotted versus the EIT cooling time. The black dotted line is an exponential fit to the data. The blue curve shows the average cooling transient computed for single ions. To approximately incorporate the radial crystal structure, we compute single-ion transients for each distance in the crystal from the trap center, and then average by weighting each transient by the number of ions at that radius. The stepwise behavior is an artifact caused by choosing the same initial phase of rotation for each transient. The thickness of the curve accounts for a 10% uncertainty in the powers of the EIT lasers. Inset: Simulated c.m. mode cooling transients for a single ion (blue) and a crystal with two closed shells (19 ions) (red). The cooling rate increases with ion number.

All observed line shapes agree well with the theoretical predictions, enabling temperatures to be evaluated through fits to the model [Eq. (1)]. After Doppler cooling only, occupancies consistent with the Doppler cooling limit are obtained. After EIT cooling we obtain nearly identical measurements of $\bar{n} = 0.28 \pm 0.18$ and $\bar{n} = 0.29 \pm 0.17$ with $\Phi_0 = 0$ and π, demonstrating near ground-state cooling for the c.m. mode with greater than 100 ions. The measured $\bar{n}$ is approximately 1 standard deviation higher than theory indicates is possible, for reasons that are not currently well understood.

To determine a cooling rate for the c.m. mode, we measured the c.m. mode occupation $\bar{n}$ for increasing durations of EIT cooling. Figure 3 shows measurements obtained with a $2\tau = 300$ μs ODF interaction time and the sequence employed in Fig. 2(c). The measured cooling transient can be well described by an exponential with $1/e$ time of $\tau_{\text{cool}} = 27.6 \pm 1.7$ μs. The measured heating of the c.m. mode is negligible on this timescale [21].

This measured cooling rate is faster than the average rate expected from N independently cooled ions (blue curve in Fig. 3). This observation is consistent with detailed numerical simulations of EIT cooling with smaller crystals, where the cooling rate of the c.m. mode is found to increase with N [15]. The inset of Fig. 3 shows simulated transients for the c.m. mode for a single ion and a 19-ion crystal, demonstrating an increase in cooling rate with the number

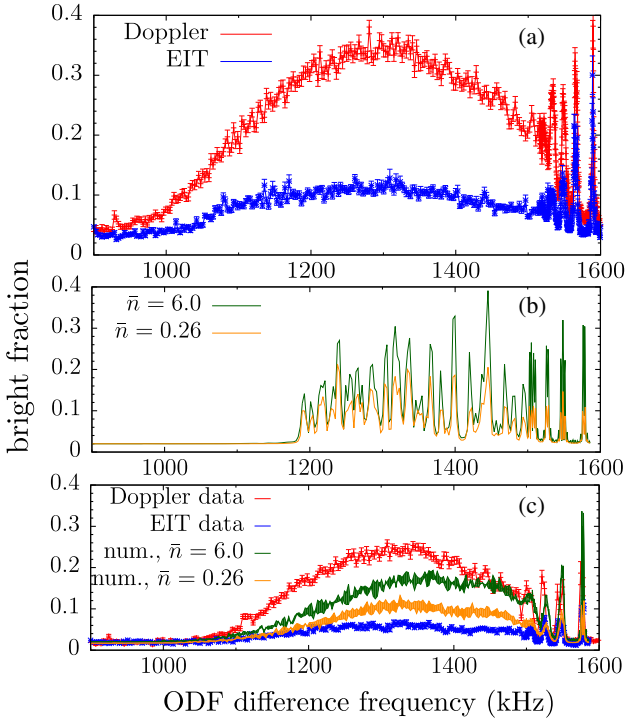

FIG. 4. Scan over all the axial drumhead modes. (a) Data taken after Doppler cooling (red) and after Doppler and EIT cooling for 200 μs (blue) for a crystal with 158 ± 10 ions. (b) Theoretical calculation of the bright fraction for a crystal with $N = 79$ ions after Doppler cooling (green) and subsequent EIT cooling (orange). (c) Comparison of the measured (red, blue) and the theoretically calculated (green, orange) bright fraction for a crystal with $N = 79 \pm 5$ ions and $t_{\mathrm{EIT}} = 300$ μs. The calculation took into account mode frequency instabilities leading to the loss of visibility of individual modes, and a 5% uncertainty in the ODF amplitude F.

of ions. The simulations also reproduce the experimentally observed initial heating during the first few microseconds, as the $N = 19$ curve in the inset shows. The initial heating is caused by transient internal transitions until the ions reach the approximate dark state.

EIT cooling enables simultaneous cooling of all the drumhead modes without changing experimental parameters. Figure 4(a) shows spin-dephasing measurements as the ODF difference frequency is swept over the full drumhead mode bandwidth of a crystal with $N = 158 \pm 10$ ions after only Doppler cooling (red), and after Doppler cooling followed by 200 μs of EIT cooling (blue). The significant reduction in the bright fraction over the entire bandwidth after EIT cooling suggests substantial sub-Doppler cooling of all the drumhead modes, even for large N.

An analysis of the drumhead mode temperatures is less challenging for smaller numbers of ions. Figures 4(b) and 4(c) summarize an investigation of the drumhead mode temperatures for a smaller crystal with $N = 79$ ions. Figure 4(b) shows a theoretical calculation of the bright fraction using Eq. (1) with an ODF interaction time $2\tau = 600$ μs, where all modes are assumed to have a uniform occupation with $\bar{n} = 6$ (green, Doppler cooling) and $\bar{n} = 0.26$ (orange, EIT cooling). The calculation assumes stable mode frequencies and indicates that for the parameters of the measurement the modes should be partially resolved. This is to be contrasted with Fig. 4(c), which shows experimental scans over the drumhead mode bandwidth of an $N = 79 \pm 5$ ion crystal after only Doppler cooling (red) and after subsequent EIT cooling (blue). For the latter we quantitatively measure the mean occupation of the c.m. mode to be $\bar{n} = 0.26 \pm 0.38$. As in Fig. 4(a), a partially resolved mode structure is only observed for the highest frequency drumhead modes.

We attribute this lack of structure to mode frequency fluctuations, which may arise from microscopic rearrangements of the ion crystal over the many repetitions of the experiment, or from damping due to coupling between modes. We expect frequency fluctuations from these sources to increase with decreasing wavelength, which in general corresponds to decreasing drumhead mode frequency. In Fig. 4(c), we plot the theoretical bright fraction (green, orange) for the crystal used in Fig. 4(b), but now incorporating mode frequency fluctuations. Our model assumes Gaussian fluctuations that increase linearly from 1 kHz for the second-highest frequency mode to a maximum fluctuation, which in Fig. 4(c) is set to 80 kHz, for the lowest frequency mode.

By comparing our theoretical model to the experimental data, we make qualitative assessments of the temperature and the frequency fluctuations of the drumhead modes. The similar spectra for the numerically computed $\bar{n} = 0.26$ bright fraction (orange) and the experimentally observed EIT-cooled spectrum (blue) in Fig. 4(c) strongly suggests near ground-state EIT cooling for all the drumhead modes as well as fluctuations of tens of kHz for the low frequency drumhead modes. A more quantitative determination of the EIT-cooled temperatures in the future will require an improved understanding of the mode frequency fluctuations and the impact of the fluctuations on the spin-spin interaction signal that is dominant at low temperatures. For the case of only Doppler cooling, the data (red) and theoretical model (green) agree well for the higher frequency modes, but are not qualitatively similar at low frequencies. Possible reasons include significantly higher occupations than $\bar{n} = 6$, beyond Lamb-Dicke effects that our model does not capture, and coupling with other modes, which might increase the spin dephasing that dominates at higher temperatures. Improved modeling that includes some of these effects may enable a more quantitative analysis in the future.

In conclusion, we have demonstrated near ground-state EIT cooling of the entire bandwidth of drumhead modes of large planar ion crystals in a Penning trap. Fast cooling rates and very low steady-state occupations enable EIT cooling to quickly initialize the axial modes to very low

temperatures, thereby greatly improving the quality of quantum simulation and quantum metrology protocols. This result greatly increases the ion crystal size and number of phonon modes that can be cooled near to the ground state. Future work will study whether EIT cooling could be employed for ground-state cooling for three-dimensional crystals with much larger numbers of ions.

We thank M. J. Affolter, Y. Lin, J. Cooper, R. J. Lewis-Swan, S. S. Kotler, and J. D. Teufel for stimulating discussions. We thank J. W. Britton and B. C. Sawyer for the help with preparatory work in the lab. We acknowledge the use of the Quantum Toolbox in PYTHON (QuTiP) [32,33] for the single-ion calculations in the main panel of Fig. 3. This work was supported by NSF Grants No. PHY 1734006 and No. PHY 1820885, DARPA Extreme Sensing, the Air Force Office of Scientific Research Grants No. FA9550-18-1-0319 and its Multidisciplinary University Research Initiative grant (MURI), Army Research Office Grant No. W911NF-16-1-0576, JILA-NSF Grant No. PFC-173400, and the National Institute of Standards and Technology (NIST). E. J. gratefully acknowledges the Leopoldina Research Fellowship, German National Academy of Sciences Grant No. LPDS 2016-15, and the NIST-PREP program. This manuscript is a contribution of NIST and not subject to U.S. copyright.

*elena.jordan@nist.gov

[1] S. Peil and G. Gabrielse, Phys. Rev. Lett. **83**, 1287 (1999).
[2] F. Diedrich, J. C. Bergquist, W. M. Itano, and D. J. Wineland, Phys. Rev. Lett. **62**, 403 (1989).
[3] H. Perrin, A. Kuhn, I. Bouchoule, and C. Salomon, Europhys. Lett. **42**, 395 (1998).
[4] M. Hofheinz, M. Ansmann, R. C. Bialczak, M. Lenander, E. Lucero, M. Neeley, D. Sank, H. Wang, M. Weides, J. Wenner, J. M. Martinis, and A. N. Cleland, Nature (London) **464**, 697 (2010).
[5] J. D. Teufel, T. Donner, D. Li, J. W. Harlow, M. S. Allman, K. Cicak, A. J. Sirois, J. D. Whittaker, K. W. Lehnert, and R. W. Simmonds, Nature (London) **475**, 359 (2011).
[6] J. Chan, T. P. M. Alegre, A. H. Safavi-Naeini, J. T. Hill, A. Krause, S. Gröblacher, M. Aspelmeyer, and O. Painter, Nature (London) **478**, 89 (2011).
[7] B. E. King, C. S. Wood, C. J. Myatt, Q. A. Turchette, D. Leibfried, W. M. Itano, C. Monroe, and D. J. Wineland, Phys. Rev. Lett. **81**, 1525 (1998).
[8] G. Stutter, P. Hrmo, V. Jarlaud, M. K. Joshi, J. F. Goodwin, and R. C. Thompson, J. Mod. Opt. **65**, 549 (2018).
[9] G. Morigi, J. Eschner, and C. H. Keitel, Phys. Rev. Lett. **85**, 4458 (2000).
[10] G. Morigi, Phys. Rev. A **67**, 033402 (2003).
[11] C. F. Roos, D. Leibfried, A. Mundt, F. Schmidt-Kaler, J. Eschner, and R. Blatt, Phys. Rev. Lett. **85**, 5547 (2000).
[12] Y. Lin, J. P. Gaebler, T. R. Tan, R. Bowler, J. D. Jost, D. Leibfried, and D. J. Wineland, Phys. Rev. Lett. **110**, 153002 (2013).
[13] K. Xia and J. Evers, Phys. Rev. Lett. **103**, 227203 (2009).
[14] R. Lechner, C. Maier, C. Hempel, P. Jurcevic, B. P. Lanyon, T. Monz, M. Brownnutt, R. Blatt, and C. F. Roos, Phys. Rev. A **93**, 053401 (2016).
[15] A. Shankar, J. E. Jordan, K. A. Gilmore, A. Safavi-Naini, J. J. Bollinger, and M. J. Holland, Phys. Rev. A **99**, 023409 (2019).
[16] J. W. Britton, B. C. Sawyer, A. C. Keith, C.-C. Joseph Wang, J. K. Freericks, H. Uys, M. J. Biercuk, and J. J. Bollinger, Nature (London) **484**, 489 (2012).
[17] M. Gärttner, J. G. Bohnet, A. Safavi-Naini, M. L. Wall, J. J. Bollinger, and A. M. Rey, Nat. Phys. **13**, 781 (2017).
[18] K. A. Gilmore, J. G. Bohnet, B. C. Sawyer, J. W. Britton, and J. J. Bollinger, Phys. Rev. Lett. **118**, 263602 (2017).
[19] B. Lounis and C. Cohen-Tannoudji, J. Phys. II (France) **2**, 579 (1992).
[20] In the room-temperature vacuum system, inelastic collisions with the H_2 background gas slowly converts Be^+ ions to BeH^+ molecular ions that centrifugally separate to the radial edge of the crystal. For the measurements discussed here the number of impurity ions was less than $\lesssim 20\%$ of the total N.
[21] See Supplemental Material at http://link.aps.org/supplemental/10.1103/PhysRevLett.122.053603 for detailed information about the experimental setup and parameters, a discussion of possible origins of the mode frequency fluctuations, and a derivation of the expression used to extract temperatures, which includes Refs. [22–26].
[22] W. M. Itano, J. C. Bergquist, J. J. Bollinger, J. M. Gilligan, D. J. Heinzen, F. L. Moore, M. G. Raizen, and D. J. Wineland, Phys. Rev. A **47**, 3554 (1993).
[23] F. Bolton and U. Rössler, Superlattices Microstruct. **13**, 139 (1993).
[24] L. R. Brewer, J. D. Prestage, J. J. Bollinger, W. M. Itano, D. J. Larson, and D. J. Wineland, Phys. Rev. A **38**, 859 (1988).
[25] S. L. Gilbert, J. J. Bollinger, and D. J. Wineland, Phys. Rev. Lett. **60**, 2022 (1988).
[26] M. L. Wall, A. Safavi-Naini, and A. M. Rey, Phys. Rev. A **94**, 053637 (2016).
[27] B. C. Sawyer, J. W. Britton, and J. J. Bollinger, Phys. Rev. A **89**, 033408 (2014).
[28] J. G. Bohnet, B. C. Sawyer, J. W. Britton, M. L. Wall, A. M. Rey, M. Foss-Feig, and J. J. Bollinger, Science **352**, 1297 (2016).
[29] S. B. Torrisi, J. W. Britton, J. G. Bohnet, and J. J. Bollinger, Phys. Rev. A **93**, 043421 (2016).
[30] C.-C. Joseph Wang, A. C. Keith, and J. K. Freericks, Phys. Rev. A **87**, 013422 (2013).
[31] B. C. Sawyer, J. W. Britton, A. C. Keith, C.-C. Joseph Wang, J. K. Freericks, H. Uys, M. J. Biercuk, and J. J. Bollinger, Phys. Rev. Lett. **108**, 213003 (2012).
[32] J. Johansson, P. Nation, and F. Nori, Comput. Phys. Commun. **184**, 1234 (2013).
[33] J. Johansson, P. Nation, and F. Nori, Comput. Phys. Commun. **183**, 1760 (2012).